Journal of Sedimentary Research

Journal of Sedimentary Research, 2018, v. 88, 276–289
Research Article
DOI: http://dx.doi.org/10.2110/jsr.2018.12

QUANTIFYING ROUNDNESS OF DETRITAL MINERALS BY IMAGE ANALYSIS: SEDIMENT TRANSPORT, SHAPE EFFECTS, AND PROVENANCE IMPLICATIONS

ALBERTO RESENTINI, SERGIO ANDÒ, AND EDUARDO GARZANTI
Laboratory for Provenance Studies, Department of Earth and Environmental Sciences, University of Milano-Bicocca, Milano 20126, Italy
e-mail: alberto.resentini@unimib.it

ABSTRACT: In this article we develop a mathematical method based on image analysis to measure the textural properties of heavy minerals in fluvial, eolian-dune, and beach sediments throughout the 1800-km-long Orange cell of littoral sand transport, the longest documented so far on our planet. We analyzed the grain size and shape of 12,700 grains, including all major heavy-mineral species contained in 22 selected samples collected along the Atlantic coast, from Namibia to southern Angola. In this unique natural laboratory, where the Orange River represents a single dominant sediment source characterized by diagnostic compositional fingerprints, hyperarid climate ensures limited chemical alteration of even unstable ferromagnesian minerals.

This case study led us to: a) monitor changes in grain size and roundness of various detrital minerals during ultralong transport in high-energy shallow-marine and eolian environments; b) determine the relative durability of various detrital minerals to mechanical wear as a function of their mineralogical properties (e.g., hardness, cleavability); c) compare roundness of grains in sands of different facies to establish the relative efficiency of mechanical processes as a function of depositional environment and transporting medium (i.e., water versus air); d) compare roundness of the same detrital species in beach deposits enriched in heavy minerals to different degrees and evaluate whether rounded grains are preferentially entrained or left behind during high-energy storm events; e) test the use of textural properties to distinguish between coarser or angular grains of local provenance from smaller or rounded grains derived from distant sources. The rigorous definition of particle shape and the measurement of grain roundness is a necessary step to achieve a full understanding of sedimentary processes, evaluate mechanical effects during long-distance transport, challenge untested assumptions, and obtain useful complementary information on sediment provenance.

INTRODUCTION

Studies of natural fluvial systems have long documented that sediment transport prolonged even over a few thousands of kilometers is unable to significantly modify the mineralogical composition or the shape of sand-size detrital minerals (e.g., Russell and Taylor 1937; Shukri 1950; Breyer and Bart 1978). Nevertheless, the opposite view has long been espoused by the sedimentological community, and many remained inclined to believe in the effectiveness of mechanical processes. Commonly taught in undergraduate courses is that rounded grains must have travelled over a long distance, whereas angular ones should be derived locally. Among detrital components, not only shale/slate or carbonate grains are largely held to be labile (McBride and Picard 1987; Garzanti 2017), but also volcanic rock fragments and mafic minerals (Blatt 1978; Ingersoll et al. 1993) or even feldspars (Dutta et al. 1993; McBride et al. 1996) are often considered unfit to survive sediment transport. Mere plausibility is, however, unacceptable as a scientific criterion (Russell 1937), and multiple experimental observations are needed to corroborate a theory (Chapter 10 in Popper 1959).

A most suitable location to test the effect of prolonged mechanical wear on detrital minerals is the Atlantic coast of southern Africa, where intense physical processes are coupled with minimum intensity of chemical processes, ultralong-distance sediment transport takes place in both shallow-marine and eolian environments, and one compositionally distinct sediment source is present, thus minimizing the uncertainties associated with mixing and dilution effects. In such an exceptional natural laboratory we have evaluated the progressive change in size and roundness and the relative durability, roundability, and rollability of heavy minerals, and investigated the provenance implications of anomalous textural relationships both among different and within single sand samples. This article illustrates a mathematical method to measure grain roundness and demonstrates the usefulness of quantitative textural data for a better understanding of sedimentological processes and for more accurate environmental and provenance reconstructions.

ROUNDNESS OF DETRITAL GRAINS

Despite their importance in understanding sedimentary processes such as mechanical abrasion, weathering, and hydraulic sorting (Pettijohn et al. 1973, p. 81), and also for industrial or commercial purposes (e.g., Dill 2007; Sun 2009; Xia 2017), shape properties have received much less attention than size studies mainly because their measurement is long, tedious, and imprecise (Russell and Taylor 1937; Curray and Griffiths 1955; Folk 1955).

Published Online: February 2018
 1527-1404/18/088-276/$03.00

Original Definitions of Grain Roundness

Roundness, an aspect of grain shape not to be confused with sphericity (Krynine 1956; Sneed and Folk 1958), is the estimated smoothness of the surface of a grain. Roundness, first measured quantitatively on cobbles as the ratio of the radius of curvature of the most convex part of the surface to half of the longest diameter through that point (Wentworth 1919, p. 517), was redefined as the average radius of curvature of all corners of the grain in one plane divided by the ratio of the largest inscribed circle in that plane (Wadell 1932, p. 448; Krumbein 1940, p. 670). Dobkins and Folk (1970) suggested instead the ratio between the radius of the sharpest corner to the radius of the largest inscribed circle. A perfectly smooth sphere has thus a roundness of 1. Such measures are, however, impractical, and roundness is thus generally—and more readily although rather inaccurately—estimated by comparison with sets of images.

The standard chart prepared by Krumbein (1941) has nine subdivisions, whereas Powers (1953) proposed a photographic scale based on two sets of grains with different sphericity. The equivalence between Krumbein's and Powers's scales is determined visually as follows: 0.1 = very angular; 0.2 = angular; 0.3 = subangular; 0.5 = subrounded; 0.7 = rounded; 0.9 = well rounded. Folk (1955) suggested for roundness intervals a logarithmic ρ scale analogous to the ϕ scale for size, with the following correspondence to Powers's and Wadell's scales: very angular = 0.12–0.17 = $\rho < 1$; angular = 0.17–0.25 = $1 < \rho < 2$; subangular = 0.25–0.35 = $2 < \rho < 3$; subrounded = 0.35–0.49 = $3 < \rho < 4$; rounded = 0.49–0.70 = $4 < \rho < 5$; well rounded = 0.7–1.0 = $5 < \rho < 6$. A perfectly smooth sphere would have a roundness of 6 ρ. The concept of roundness sorting can be expressed by the roundness standard deviation σ_ρ. Folk (1980, p. 10) indicated the following classes for roundness sorting: very good $\sigma_\rho < 0.6$; good $0.6 < \sigma_\rho < 0.8$; moderate $0.8 < \sigma_\rho < 1.0$; poor $1.0 < \sigma_\rho < 1.2$; very poor $\sigma_\rho > 1.2$.

How to Measure Grain Roundness?

Measuring textural properties in clastic sediments, including sorting, sphericity, or roundness, is complex, time-consuming, and imprecise (Clark 1981; Beddow 1986; Diepenbroek et al. 1992). A traditional semiquantitative approach is based on the visual comparison with bidimensional or tridimensional standard charts (Folk 1951; Terry and Chilingar 1955; Harrell 1984; Jerram 2001). Silhouette charts for roundness were among the first to be proposed (Krumbein 1941; Powers 1953), but the results obtained are somewhat empirical and subjective (Fig. 1).

An objective quantitative technique based on Fourier series was developed subsequently by Ehrlich and Weinberg (1970; Thomas et al. 1995; Bowman et al. 2000), by which the shape of two-dimensional grain outlines is decomposed into a series of shape harmonics. Lower-order harmonics measure grain shape (sphericity), whereas higher-order harmonics measure small-scale irregularities (roughness or angularity, which is the reciprocal of roundness). Grains characterized by complex crenellate-edge or re-entrant morphology with deep embayments cannot be resolved.

Technologists in powder and fine-particle studies tackled these problems by converting particle profiles into sets of Fourier coefficients (Beddow et al. 1977; Luerkens 1991). Alternatively, the geometry of very irregular profiles can be described mathematically by their fractal dimension (Mandelbrot 1977; Kaye 1978; Whalley and Orford 1989), a complementary approach that can be used in sedimentology to quantify the angularity of detrital grains (Orford and Whalley 1983; Hyslip and Vallejo 1997). A mathematical relationship with Krumbein's roundness values was established by Vallejo and Zhou (1995), and results obtained by visual estimates and automated methods were compared numerically by Hryciw et al. (2016).

Technological progress with the recent introduction of QemScan, mineral liberation analysis, or Raman spectroscopy allows an efficient identification of large sets of grains, but not all equipment incorporates devices specifically dedicated to image analysis (e.g., Malvern Morphologi G3-ID). The extensive use of computer programs leads to a mathematical redefinition of textural parameters, which on the one hand becomes precise and objective, but on the other hand hardly equivalent to those defined in classical sedimentology. Typical output parameters include "circularity" (a two-dimensional proxy for sphericity calculated as 4π times the square of the area divided by the square of the perimeter) and a parameter unfortunately called "roundness" (calculated as four times the area divided by π times the long axis; Cox and Budhu 2008), which represents the inverse of the elongation (Rasband 1997). "Roundness" thus defined does not provide any useful information on grain roundness. Despite all theoretical efforts and great technological progress made in computer-based image analysis, a fully satisfactory automatic method to quantify the angularity of detrital particles is yet to be found (Raadnui 2005; Tafesse et al. 2013).

A NOVEL APPROACH TO ROUNDNESS ANALYSIS

In this study we propose two alternative methods to quantify grain roundness on bidimensional digital images using Matlab® routines. The first approach is based on Fourier descriptors calibrated with classical visual-comparison charts. The second approach stems from the original definition by Wadell (1932), and considers the radius of curvature of corners relative to the radius of the maximum inscribed circle (Fig. 2).

Image analysis is carried out on digital photographs taken with the optical microscope (objectives 4× and 10×, parallel polarizers, camera resolutions 2048 × 1536 and 3264 × 1836 pixels) and including a micrometric reference scale. Grain outlines are extracted by a region-competition image-segmentation algorithm (Cardinale et al. 2012), and the graphical output is visually checked grain by grain for consistency. Grains in point contact were separated, and overlapping grains were not considered wherever grain boundaries were not evident. For each grain, the full array of size and shape parameters—including long and short axes, perimeter, and area—is determined by the software after converting from pixels to micrometers. Grain size is calculated as the geometric mean of the short and long axes (equivalent diameter), and sphericity as the ratio between the short and long axes (Folk 1980, p. 9). Sorting values and classification are after Folk (1980, p. 42). The mineralogy of each numbered grain is finally identified under the microscope, allowing us to quantify the morphological features of each heavy-mineral species. Such a grain-counting procedure also allows us to compare the obtained number frequencies with the volume percentages assessed by point counting on the same samples. The size differences between detrital minerals in ϕ units ("size shifts") as determined by image analysis are combined with grain-size data on the bulk sediment to perform settling-equivalence analysis (Garzanti et al. 2008).

The Fourier Descriptor

Grain roundness is first evaluated by visual comparison with classical charts (Krumbein 1941; Powers 1953), and next quantified by Fourier analysis (Nixon and Aguado 2002). Both lowest-order and highest-order Fourier components are discarded to define the surface roughness of grain outlines accurately, the former accounting for the general grain shape and the latter being unduly influenced by the limited resolution of the image. By applying Fourier analysis to all grains illustrated in the Krumbein's roundness chart, we found an optimal linear correlation with Krumbein's roundness values (R^2 0.85) when using the sum from the 4th to the 30th Fourier coefficients (defined as $\sum_4^{30} RDN$). The $\sum_4^{30} RDN$ values measured for each detrital grain are converted into Krumbein's scale

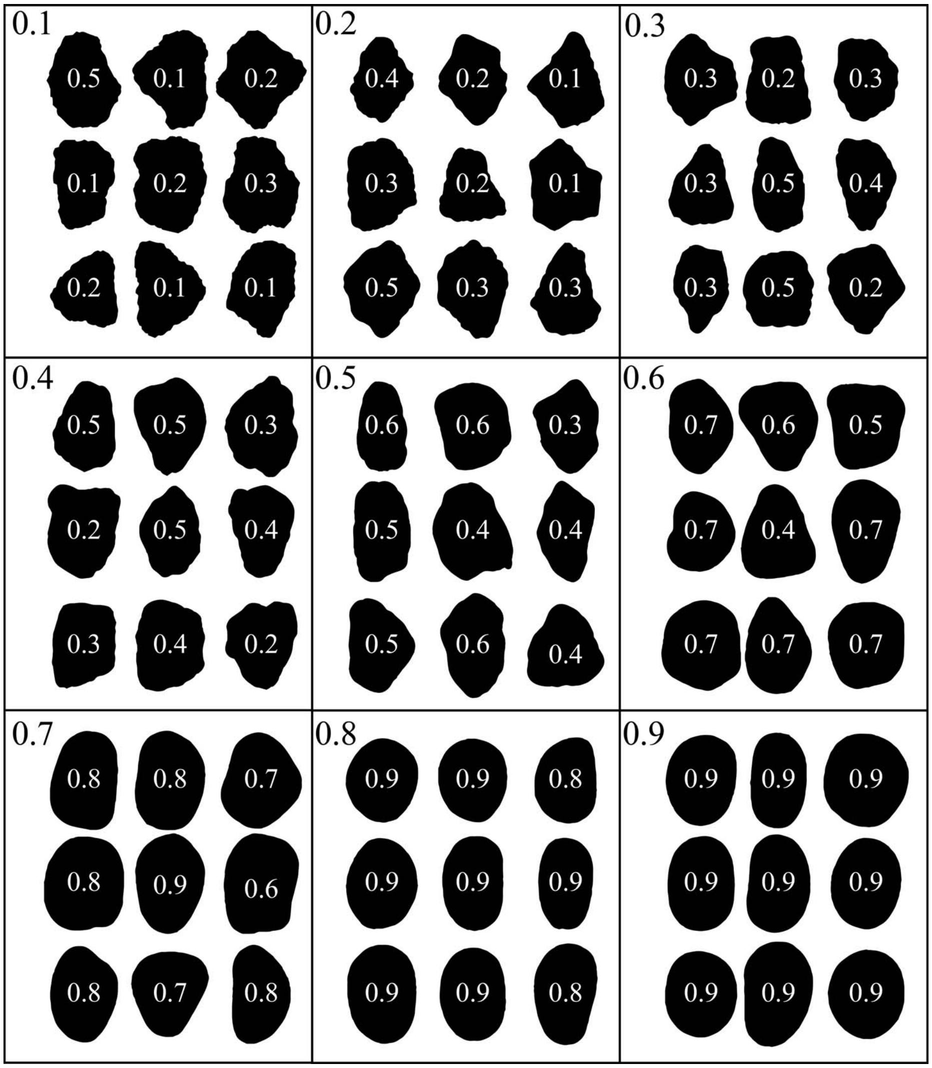

FIG. 1.—Visual definition of roundness. Krumbein's (1941) chart contains 81 grains subdivided empirically in 9 classes of increasing values from 0.1 to 0.9. The values shown for each grain are calculated with the Fourier method [$\sum_4^{30} RDN$ converted into Krumbein's scale according the linear relationship (0.36 – $\sum_4^{30} RDN$) / 0.275]. Note that 15% of total grains are misclassified by more than one class.

according the optimal linear relationship (0.36 – $\sum_4^{30} RDN$) / 0.275. Such numerical conversion allowed us to rearrange the original chart of Krumbein's (1941) in a new revised chart that for each class includes selected grains yielding consistent values, thus providing an upgraded version of a tool that has been widely used by generations of students for the visual determination of grain roundness (Fig. 3).

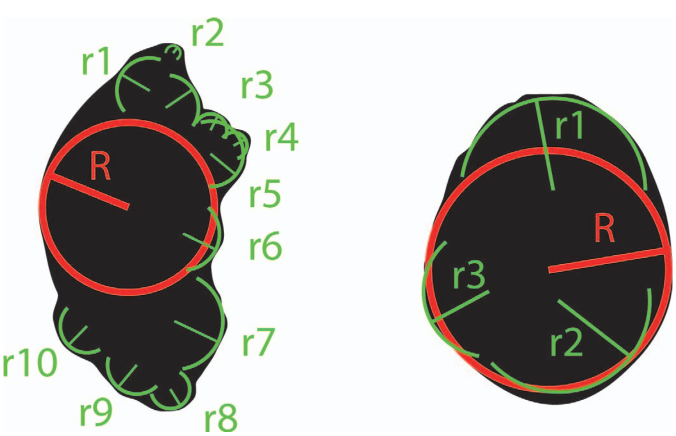

FIG. 2.—Geometrical definition of roundness. According to Wadell (1932), roundness is calculated as the ratio between the average of the radii of circles inscribed in corners (green) and the radius of the maximum inscribed circle (red).

The Wadell Method

Grain roundness can be quantified as the ratio between the mean radius of curvature of the corners and the radius of the largest inscribed circle (Leeder 1982, p. 41), a value which is impractical to measure unless an automated procedure is used (Zheng and Hryciw 2015). Our Matlab® routine calculates, for each mineral grain contained in a binary image, the radius of circles inscribed in grain corners and the radius of the maximum inscribed circle. To minimize the fictitious angularity generated by the pixel effect—as well as the time required for analysis—vertices are reduced for each grain to the minimum number required to preserve its area and shape. For each selected vertex, the routine calculates the radius of the circle that best fits the portion of the grain outline including two adjacent vertices on each side by using the geometrical approximation of Taubin (1991). All circles larger than the maximum inscribed circle or having their centers external to the grain are not considered. Grain roundness is finally obtained as the arithmetic mean of the ratios between the radius of the circle inscribed in each corner and the radius of the maximum inscribed circle (Fig. 4). Roundness is thus comprised between 0 and 1 as in Wadell (1932).

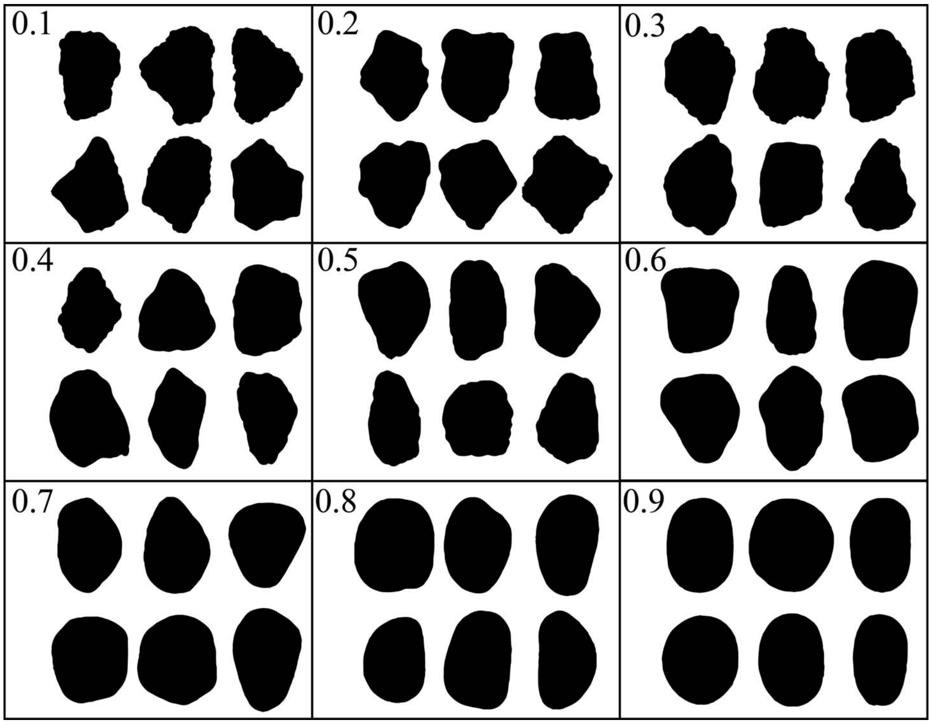

FIG. 3.—Upgraded Krumbein's (1941) chart to be used for a more accurate visual determination of grain roundness. This revised visual chart contains 54 selected grains rearranged in their proper class according to the values calculated with the Fourier method.

THE ORANGE CELL TEXTURAL CASE: OBSERVATIONS

In this section we describe the textural properties of all major heavy-mineral species found in river, dune, beach, and beach-placer sands throughout the 1800-km-long Orange cell of longshore sand transport, thus documenting the effects of physical processes on sediment texture and mineralogy (Fig. 5). In this stretch of the Atlantic coast extending from Namibia to southern Angola, unique features most suitable for carrying out such an experiment include: a) presence of one major compositionally distinct sediment source; b) few, subordinate, and well identified additional entry points of detritus; c) hyperarid climate with consequently negligible chemical weathering; d) high-energy eolian and shallow-marine environments; and, e) strong hydraulic-sorting effects and deposition of beach and dune sands enriched in heavy minerals to markedly different degrees (i.e., "placers" versus "semi-placers," "neutral sands," and "anti-placers;" Garzanti et al. 2012, 2014, 2017a). During several field campaigns between 2007 and 2016, sand samples were collected from active river bars, beach berms, and eolian dunes. In order to avoid anomalous local enrichments in heavy minerals, samples were collected invariably on the crests of the largest dunes and, in beaches, away from areas where ultradense minerals were concentrated by selective-entrainment processes. Such hydrodynamic effects were specifically investigated by separately collecting garnet and magnetite placers on the foreshore of Namib beaches.

Long-Distance Grain-Size Trends

Grain-size measurements on 48 bulk samples, carried out both in thin section by ranking and visual comparison with sieved standards and by laser granulometry, failed to document any significant trend from south to north along the Orange littoral cell (Garzanti et al. 2015a). Orange River samples range in mean grain size from 110 μm to 400 μm. Beach samples range mostly from 170 to 400 μm in the Namib Erg and from 170 and 350 μm in the Moçamedes Desert. Dune samples range mostly from 180 and 390 μm in the Coastal Namib Erg, decrease northward from 370 to 240 μm in the Skeleton Coast Erg, and range from 200 and 330 μm in the Moçamedes Desert.

Grain-size measurements by image analysis on 22 samples confirm the lack of northward grain-size decrease. The relative size of different minerals are chiefly controlled by the settling-equivalence principle and equally fail to identify systematic fining trends with transport distance (Fig. 6).

Long-Distance Roundness Trends

We measured grain roundness with both Fourier and Wadell methods on all heavy-mineral species identified in 22 selected samples, including abundant clinopyroxene and opaque Fe-Ti-Cr oxides, common garnet, amphibole, and epidote, and less common zircon, hypersthene, staurolite, apatite, rutile, and monazite. Roundness determinations indicate a rapid northward increase in roundness for all heavy minerals from the Orange River mouth to the Coastal Namib Erg, documenting a prominent effect of mechanical wear. Roundness values do not increase farther northward, also because more angular detritus is supplied by local rivers (Figs. 7, 8). For instance, average roundness of clinopyroxene grains increases rapidly from 0.21 (Fourier method) and 0.59 (Wadell method) in Orange River samples up to 0.71 and 0.74 in northern Coastal Namib dunes, and next remains broadly constant from 0.74 and 0.72 in northern Namib beaches to 0.73 and 0.72 in Moçamedes beaches (Table 1). Values calculated with the two methods are different but display the same trend (Figs. 7, 8). The Fourier method yields much lower values on angular sands and values only slightly lower than or similar to the Wadell method on rounded sands; much lower variability is thus obtained with the Wadell method (Table 1).

Grain-Size Relationships among Detrital Minerals

Based on the settling-equivalence principle, Fe-Ti-Cr oxide grains (average density 5.0 g/cm^3) are expected to be 0.42 to 0.57 ϕ finer than clinopyroxene grains (density 3.3 g/cm^3) in fine to medium sands

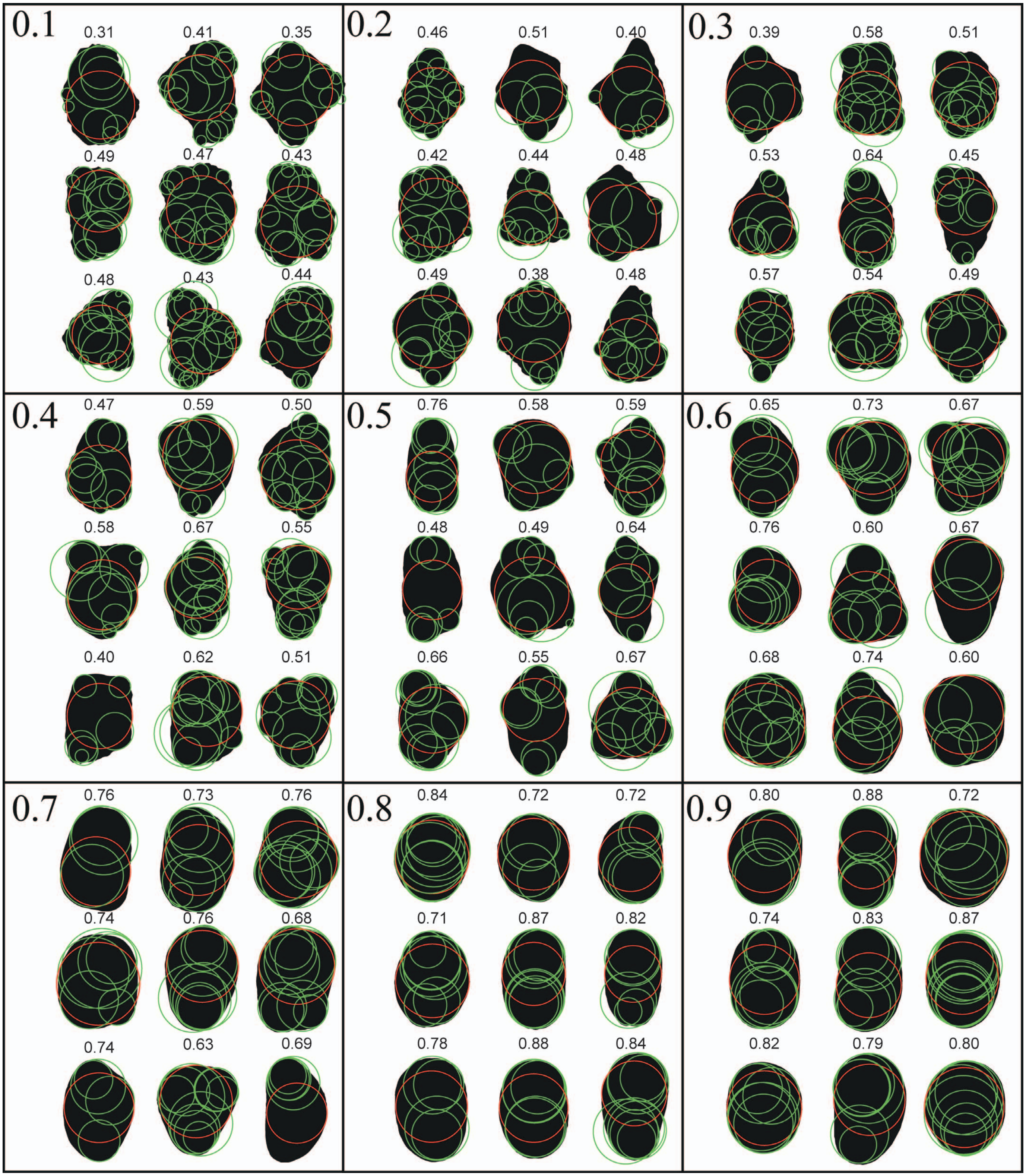

FIG. 4.—Comparison of Wadell's (1932) and Krumbein's (1941) approaches for measuring roundness (Krumbein's values shown in upper left corner of each panel, Wadell's values given for each grain). The marked discrepancies result from both different operational definitions and imprecise classification of grains in Krumbein's (1941) visual chart.

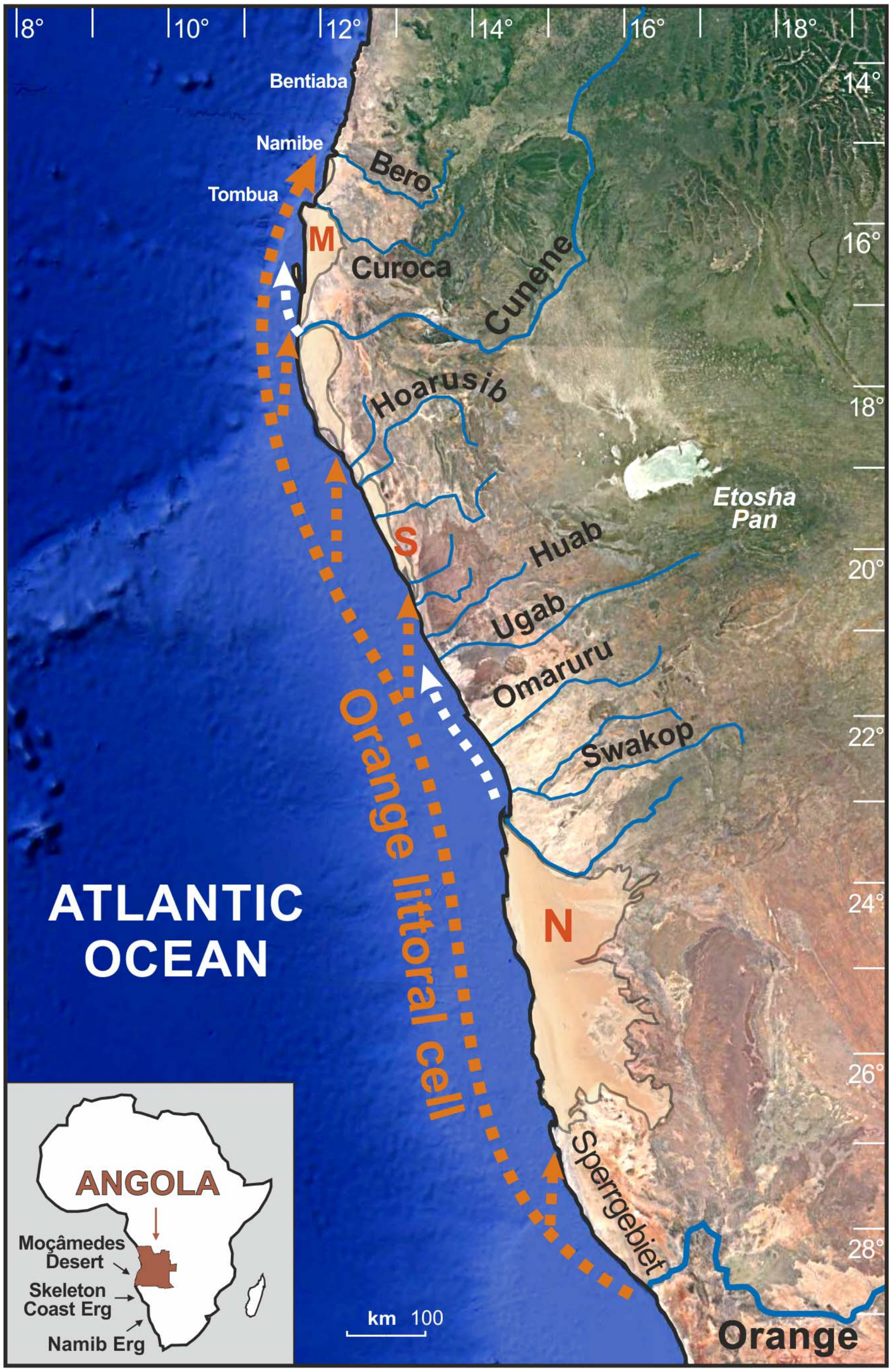

FIG. 5.—The 1800-km-long cell of littoral transport along the Atlantic coast of southern Africa (white arrows indicate the only two significant entry points of detritus beside the Orange, Swakop, and Cunene rivers). The Coastal Namib Desert (N) is almost entirely fed with sand dragged long-distance by persistent swell waves from the Orange mouth, and can thus be considered as its wave- and wind-displaced delta (Rogers 1977; Garzanti et al. 2012). Dune sand in the Skeleton Coast Erg (S) is supplied ca. 80% from the Orange and ca. 20% from the Swakop and other ephemeral rivers draining the Damara orogen in central Namibia (Garzanti et al. 2014). Beach and dune sand in the Moçamedes Desert farther north (M) is calculated to be derived 55–60% from the Orange, 15–20% from the Swakop and other Namibian rivers, and 20–25% from the Cunene River (Garzanti et al. 2017a).

deposited by tractive currents in water or air (Vermeesch et al. 2016). In our samples, Fe-Ti-Cr oxides are indeed consistently finer than clinopyroxene (Table 1), but commonly somewhat less than expected (mostly only 0.2 to 0.4 ϕ finer). Zircon (density 4.65 g/cm^3) and epidote (density 3.45 g/cm^3) are, respectively, 0.3–0.5 ϕ finer and about the same size as clinopyroxene, as predicted. Amphibole (density 3.2 g/cm^3) is as expected ca. 0.2 ϕ coarser than clinopyroxene throughout coastal Namibia, whereas it is ca. 0.4 ϕ coarser in Moçamedes Desert sand.

Roundness Relationships among Detrital Minerals

Garnet and staurolite are the only minerals that are subangular to subrounded even in Moçamedes Desert sands. Zircon is subrounded already in the initial tract of the Orange littoral cell, and as rounded as clinopyroxene at the end of the Orange cell. Epidote is somewhat more angular than clinopyroxene. Hypersthene is more angular than clinopyroxene in Moçamedes Desert sands. Fe-Ti-Cr oxides are more rounded than clinopyroxene in the initial tract of the Orange cell and less rounded in the

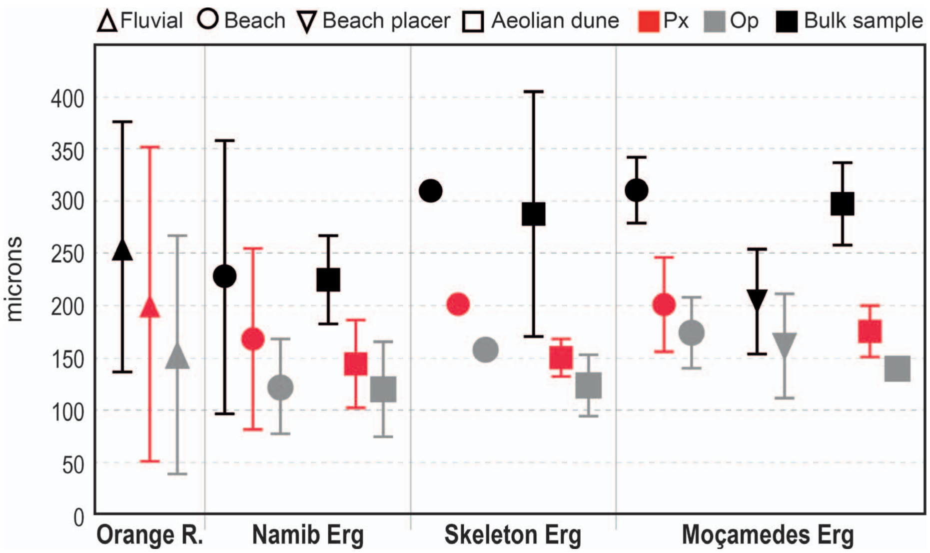

FIG. 6.—The mean grain size of bulk samples, clinopyroxene, and opaque Fe-Ti-Cr oxides remains remarkably constant in the various depositional environments throughout the Orange littoral cell. Because of the settling-equivalence principle (Rubey 1933), ultradense Fe-Ti-Cr oxides are invariably finer-grained than less dense pyroxene.

terminal tract. Amphiboles are more angular than clinopyroxene from the northern Coastal Namib to the Skeleton Coast and southern Moçamedes Desert.

Intersample Textural Variability of Moçamedes Beach Sands

At Vanesinha, all detrital minerals are much finer-grained in the magnetite-garnet beach placer than in "semi-placer" beach sand, but both garnet and Fe-Ti-Cr oxides do not show a consistent intersample difference in grain roundness, whether measured with the Fourier or the Wadell methods (Table 1). Clinopyroxene is more angular in the placer sample if measured with the Fourier method, but slightly more rounded if measured with the Wadell method. No mineral displayed significant intersample differences in roundness. In the Praia do Navio garnet-magnetite beach placer, garnet is more rounded than in less heavy-mineral-enriched beaches and much more rounded than in adjacent dunes. A similar trend is displayed by epidote but not by clinopyroxene, Fe-Ti-Cr oxides, or zircon.

THE ORANGE CELL TEXTURAL CASE: INFERENCES

The aim of this section is to show how the detailed inspection of the size, shape, and mineralogy of detrital grains combined can lead us to identify changes in mineralogy and textures ascribed to mechanical wear, to evaluate the relative durability and roundability of different detrital

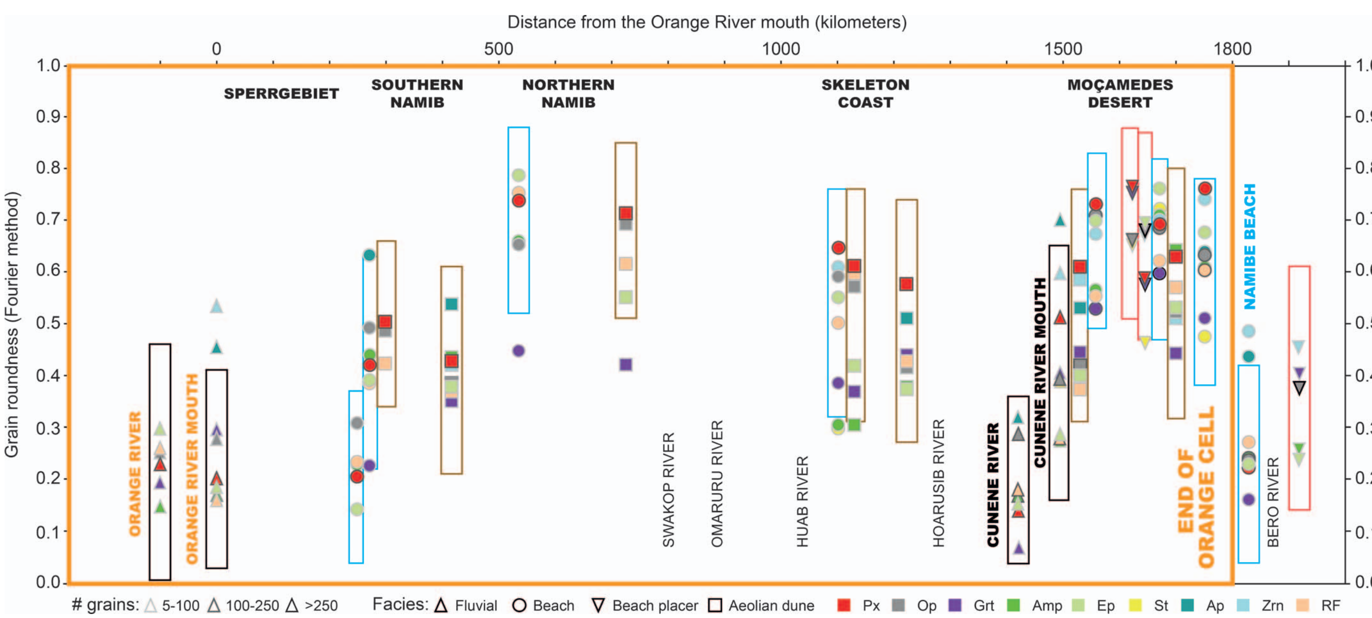

FIG. 7.—Long-distance roundness trend from the Orange River to southern Angola determined with the Fourier method. Roundness does not change during littoral transport in the Sperrgebiet, but it increases abruptly at the southern edge of the Namib Erg, pointing to the efficiency of mechanical wear in eolian environments. Heavy minerals, rounded at the northern edge of the Namib, are slightly more angular farther north owing to local contribution via the Swakop River in central Namibia and via the Cunene River in southernmost Angola, and rounded again at the northern end of the Orange littoral cell. Locally derived minerals via the Bero River in Namibe beach are angular. Boxes (outline: black for rivers, blue for beaches, red for beach placers, brown for dunes) are the envelope of the standard deviations for most abundant minerals in each sample, invariably including pyroxene (Px) and opaque Fe-Ti-Cr oxides (Op). Grt, garnet; Amp, amphibole; Ep, epidote; St, staurolite; Ap, apatite; Zrn, zircon; RF, rock fragments.

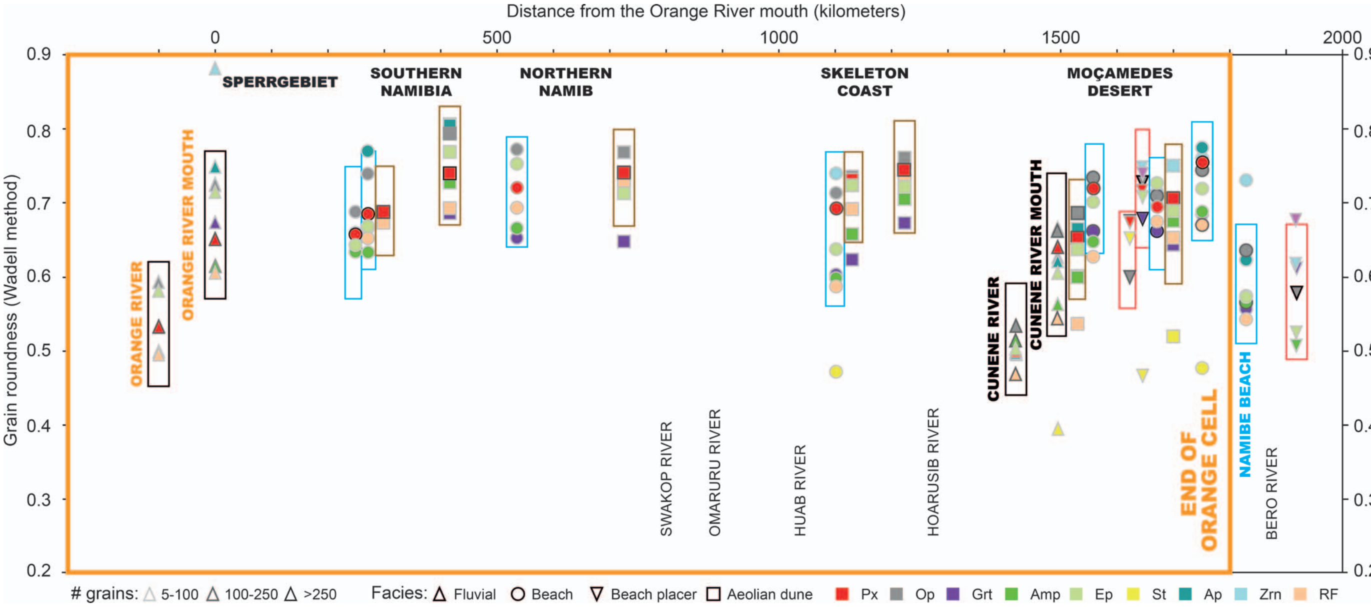

FIG. 8.—Long-distance roundness trend from the Orange River to southern Angola determined with the Wadell method. Note that, despite significant differences in the range of roundness values relative to Figure 6, the displayed trends are fully consistent. Both methods faithfully reflect changes in roundness along the Orange littoral cell. Box outlines and heavy-mineral abbreviations as in Figure 6.

minerals, to investigate shape effects, and to obtain provenance information from anomalous textural relationships.

Downdrift Fining and Long-Distance Sorting by Density

According to a popular view in sedimentology, grain size would tend to decrease in the direction of sediment transport (Russell 1939; Pettijohn et al. 1973). Downstream fining is indeed commonly observed in alluvial fans, and ascribed to either progressive pebble abrasion or decreasing slope and competence of the fluvial current (Attal and Lavé 2006; Domokos et al. 2014; Miller et al. 2014). Fining trends are not equally clear in lowland tracts of big rivers (e.g., Fig. 24 in Garzanti et al. 2015b).

In the case of longshore transport, both fining (Pettijohn and Ridge 1932; Self 1977) and coarsening (McCave 1978; Cipriani and Stone 2001) trends have been reported. Along deltaic shorelines, heavy-mineral concentration may decrease in the transport direction. This phenomenon is commonly observed where decreased sediment load leads to accelerated erosion of deltaic cusps, consequent formation of placer lags, and lateral redistribution of the selectively entrained heavy-mineral-poor sediment fraction (Frihy and Komar 1991; Li and Komar 1992; Garzanti et al. 2002, p. 15). A northward decrease in the size of detrital diamond (density 3.5 g/cm^3) is documented along the southernmost tract of the Orange littoral cell (Jacob et al. 2006; Spaggiari et al. 2006). Our results, however, fail to indicate any decrease in the grain size of beach and dune sands as of single detrital minerals, or any decline in heavy-mineral concentration, during long-distance sediment transport. On the contrary, heavy minerals concentrate markedly in the Moçamedes Desert at the end of the Orange littoral cell, where the shelf narrows and low-density minerals are selectively entrained offshore during storm events and eventually conveyed via canyons toward the deep ocean floor (Garzanti et al. 2017a).

Mechanical Breakdown and Relative Durability of Detrital Minerals

Previous studies on long-distance transport carried out in both modern settings and in the laboratory have failed to show notable mechanical effects on sediment mineralogy (Russell 1937; Shukri 1950; Nesbitt and Young 1996; Picard and McBride 2007), a notable exception being the selective destruction of least durable detrital components such as shale and slate grains in high-energy marine environments (McBride and Picard 1987; Garzanti et al. 1998, 2013). An increase in quartz during longshore transport has been ascribed to mechanical breakdown combined with tropical weathering (Savage et al. 1988), although dilution from widespread quartz-rich sources may represent an alternative explanation (McBride et al. 1996; Mehring and McBride 2007; Garzanti et al. 2015b, p. 49). Generation of quartz-rich sand through selective comminution of feldspar (Dutta et al. 1993) or carbonate rock fragments (Garzanti et al. 2017b) has received theoretical and observational support, respectively.

Mechanical breakdown of nondurable sedimentary and metasedimentary rock fragments does occur in wave-dominated high-energy environments offshore of the Orange mouth, but no clear compositional trend is displayed farther north, apart from a decrease in the amphibole/garnet ratio partly ascribed to greater cleavability and mobility of the former (Cascalho and Fradique 2007; Figs. 10 and 11 in Garzanti et al. 2015a). The only significant mineralogical changes observed along the littoral cell are caused by local addition of metamorphic and plutonic detritus derived from the Damara orogen exposed in central Namibia, including garnet, staurolite, tourmaline, and sillimanite, and from the Cunene River carrying amphibole, epidote, and hypersthene. Otherwise the proportions of heavy-mineral species do not change notably, and pyroxene grains are not selectively destroyed. Clear evidence for selective mechanical breakdown is thus lacking.

Mechanical Abrasion and Relative Roundability of Detrital Minerals

Although size reduction and roundability of carbonate grains by mechanical wear has long been documented (Wentworth 1919; Fig. 4 in Garzanti 2017), the observation of modern natural systems and laboratory experiments has shown that long-distance transport in water is unable to affect the roundness of sand grains significantly (Russell and Taylor 1937; Pettijohn 1957 p. 60; Kuenen 1959 1964). Eolian abrasion is generally held to be much more effective (Twenhofel 1945; Kuenen 1960), although the issue is somewhat controversial (Goudie and Watson 1981). Moreover,

TABLE 1.—*Grain-size and roundness values obtained by image analysis of river, dune, beach, and beach-placer sands along the Atlantic coast of southern Africa. N°, total number of measured grains per sample; Cpx, clinopyroxene; Op, opaque Fe-Ti-Cr oxides; Grt, garnet; Amp, amphibole; Ep, epidote; Zrn, zircon; Hy, hypersthene; St, staurolite; Ap, apatite; Rt, rutile; Mnz, monazite. Average density and hardness values after www.mindat.org.*

				Cpx	Op	Grt	Amp	Ep	Zrn	Hy	St	Ap	Rt	Mnz
Density	(g/cm^3)			3.30	5.00	4.00	3.20	3.45	4.65	3.40	3.75	3.20	4.25	5.20
Hardness	Mohs Scale			5.75	6.0	7.5	5.5	6.5	7.5	5.75	7.25	5.0	6.25	5.25
				GRAIN SIZE (micrometers)										
River/Site	**Facies**	**Sample**	**N°**	**Cpx**	**Op**	**Grt**	**Amp**	**Ep**	**Zrn**	**Hy**	**St**	**Ap**	**Rt**	**Mnz**
Bentiaba	placer	P4948	1930	79	72	97	95	83						
Namibe	beach	S4953	503	224	145	195	244	205	127	228		213		
Subida Grande	beach	S4954	912	178	152	173	244	198	135	276	209	164		
Tombua	dune	S4774	415	161	141	173	203	174	112	195	249			
Vanesinha	beach	S4958	623	235	200	264	318	265	174	267	263			
Vanesinha	placer	P4958	1774	72	64	73		73	58	51	73			60
P. do Navio	placer	P4959	409	126	243	164		135	202	194	199			198
S. dos Tigres	beach	S5057	510	181	170	208	238	207	160	207	198			
P. Esponjas	dune	S5056	499	189	137	190	203	143	138	159	213	149		
Cunene	mouth	S5052	721	167	154	176	258	195	132	297	173	205		
Cunene	river	S4775	488	359	300	248	258	253		288		238		
Mowe Bay	dune	S4358	216	141	106	183	143	108	100		208	119		
Torra Bay	dune	S4353	216	159	137	221	192	145						
Torra Bay	beach	S4354	393	203	157	228	230	204	133		245	226		
Walwis Bay	dune	NAM1	337	159	136	188	191	161						
Fishersbrun	beach	S4331	173	205	142	216	238	262						
South Namib	dune	S4324	801	96	72	109	108	87	75			73	75	
Lüderitz	dune	NAM12	137	150	125	141		148						
Agate	beach	S4321	633	129	105	120	161	122	90			121		
Grossebucht	beach	S4322	398	110	91	91	128	112						
Orange	mouth	NAM14A	357	112	86	111	134	91	66			113		
Orange	river	NAM13R	262	259	197	251	264	209						
				ROUNDNESS (Fourier method)										
River/Site	**Facies**	**Sample**	**N°**	**Cpx**	**Op**	**Grt**	**Amp**	**Ep**	**Zrn**	**Hy**	**St**	**Ap**	**Rt**	**Mnz**
Bentiaba	placer	P4948	1930		0.38	0.40	0.26	0.24	0.46					0.64
Namibe	beach	S4953	503	0.23	0.24	0.16	0.24	0.23	0.49	0.22		0.43		
Subida Grande	beach	S4954	912	0.77	0.64	0.51	0.60	0.68	0.74	0.54	0.48	0.60		
Tombua	dune	S4774	415	0.63	0.51	0.44	0.64	0.54	0.51	0.62	0.52			
Vanesinha	beach	S4958	623	0.69	0.69	0.60	0.70	0.76	0.70	0.60	0.73			
Vanesinha	placer	P4958	1774	0.56	0.69	0.58		0.70	0.68	0.64	0.47			0.73
P. do Navio	placer	P4959	409	0.82	0.66	0.75		0.82	0.55	0.65	0.66			0.73
S. dos Tigres	beach	S5057	510	0.73	0.71	0.53	0.56	0.70	0.68	0.69	0.47			
P. Esponjas	dune	S5056	499	0.62	0.55	0.44	0.40	0.40	0.58	0.28	0.37	0.52		
Cunene	mouth	S5052	721	0.56	0.39	0.40	0.27	0.29	0.60	0.22	0.39	0.70		
Cunene	river	S4775	488	0.15	0.29	0.07	0.18	0.16		0.13		0.31		
Mowe Bay	dune	S4358	216	0.58	0.42	0.44	0.38	0.37	0.48		0.38	0.50		
Torra Bay	dune	S4353	216	0.61	0.57	0.37	0.30	0.42						
Torra Bay	beach	S4354	393	0.65	0.59	0.39	0.30	0.55	0.61		0.30	0.51		
Walwis Bay	dune	NAM1	337	0.71	0.69	0.42	0.54	0.55						
Fishersbrun	beach	S4331	173	0.74	0.65	0.45	0.65	0.79						
South Namib	dune	S4324	801	0.42	0.37	0.35	0.44	0.36	0.42			0.53	0.45	
Lüderitz	dune	NAM12	137	0.50	0.49	0.39		0.58						
Agate	beach	S4321	633	0.42	0.49	0.23	0.44	0.39	0.64			0.63		
Grossebucht	beach	S4322	398	0.20	0.31	0.22	0.23	0.14						
Orange	mouth	NAM14A	357	0.20	0.31	0.30	0.17	0.19	0.53			0.45		
Orange	river	NAM13R	262	0.23	0.25	0.20	0.15	0.30						

TABLE 1.—*Continued.*

River/Site	Facies	Sample	N°	ROUNDNESS (Wadell method)										
				Cpx	Op	Grt	Amp	Ep	Zrn	Hy	St	Ap	Rt	Mnz
Bentiaba	placer	P4948	1930	0.68	0.61	0.51	0.53	0.62						
Namibe	beach	S4953	503	0.57	0.63	0.56	0.56	0.57	0.73	0.56		0.62		
Subida Grande	beach	S4954	912	0.75	0.75	0.68	0.69	0.72	0.77	0.66	0.64	0.77		
Tombua	dune	S4774	415	0.71	0.71	0.64	0.68	0.69	0.75	0.67	0.57			
Vanesinha	beach	S4958	623	0.70	0.71	0.67	0.70	0.72	0.71	0.68	0.69			
Vanesinha	placer	P4958	1774	0.72	0.73	0.68		0.71	0.75	0.72	0.66			0.74
P. do Navio	placer	P4959	409	0.73	0.60	0.67		0.82	0.65	0.59	0.64			0.67
S. dos Tigres	beach	S5057	510	0.73	0.74	0.66	0.65	0.70	0.72	0.68	0.63			
P. Esponjas	dune	S5056	499	0.66	0.69	0.60	0.60	0.64	0.68	0.58	0.57	0.66		
Cunene	mouth	S5052	721	0.65	0.66	0.63	0.56	0.61	0.66	0.53	0.65	0.62		
Cunene	river	S4775	488	0.47	0.53	0.50	0.51	0.50		0.50		0.57		
Mowe Bay	dune	S4358	216	0.74	0.77	0.67	0.71	0.72	0.76		0.64	0.75		
Torra Bay	dune	S4353	216	0.73	0.74	0.62	0.66	0.73						
Torra Bay	beach	S4354	393	0.69	0.71	0.60	0.60	0.63	0.74		0.57	0.71		
Walwis Bay	dune	NAM1	337	0.74	0.77	0.65	0.73	0.71						
Fishersbrun	beach	S4331	173	0.72	0.77	0.65	0.67	0.68						
South Namib	dune	S4324	801	0.74	0.80	0.69	0.73	0.77	0.81			0.80	0.80	
Lüderitz	dune	NAM12	137	0.69	0.68	0.70		0.75						
Agate	beach	S4321	633	0.69	0.74	0.67	0.63	0.67	0.79			0.77		
Grossebucht	beach	S4322	398	0.66	0.69	0.68	0.64	0.64						
Orange	mouth	NAM14A	357	0.65	0.72	0.67	0.62	0.71	0.88			0.74		
Orange	river	NAM13R	262	0.53	0.59	0.53	0.50	0.58						

grain roundness may result from wind transport as well as from recycling of rounded grains from older sandstones (Dott 2003; Muhs 2004).

Our results indicate that roundness of all detrital minerals does not change during subaqueous longshore transport in the first 300–350 km of the Orange littoral cell, whereas it increases abruptly at the transition to the eolian environment in the southern Coastal Namib (Fig. 4 in Garzanti et al. 2015a). This confirms the much greater effectiveness of grain-to-grain impacts in air than under water. In the Moçamedes Desert, detrital minerals appear to be more angular in our dune samples (Table 1), which is ascribed to the finer size of the Tombua dune and to the greater percentage of Cunene-derived angular grains in the < 20-km-long coastal stretch north of the mouth (Praia dos Esponjas dune).

More than a century ago, Mackie (1897, p. 299) observed that "*the amount of rounding is in the indirect ratio of the hardness of the mineral*." Such a relationship was confirmed by the experimental work of Marsland and Woodruff (1937), who established the following sequence of decreasing roundability: gypsum > calcite ≈ apatite > magnetite > orthoclase > quartz > garnet. With a different experiment, Dietz (1973) obtained the sequence: andalusite ≈ olivine > tourmaline ≈ staurolite > rutile ≈ garnet ≈ quartz ≈ hornblende > kyanite ≈ zircon. More recently, (Folk 1980, p. 13) specified that "*the 'roundability' of a particular mineral or rock fragment depends upon its hardness (softer grains rounding faster), and the cleavage or toughness (large grains with good cleavage tend to fracture rather than round)*."

Along the Orange littoral cell, a markedly different rate of rounding is observed for different minerals. Clinopyroxene becomes rounded at the fastest rate, followed by slightly harder Fe-Ti-Cr oxides and epidote. Amphibole has better cleavage and is systematically more angular than pyroxene. The rate of rounding is lower for harder garnet and lowest for zircon, which is already subrounded at the Orange mouth. A significant correlation at the 0.1% level is observed between roundness of most minerals measured with the Fourier method and distance from the Orange mouth (r = 0.83–0.91 for pyroxene and garnet and r = 0.66–0.71 for epidote and Fe-Ti-Cr oxides). The correlation coefficients between rounding rate and hardness of pyroxene, Fe-Ti-Cr oxides, epidote, and garnet are also significant (median $r = 0.71$ and 0.76 using the Fourier and Wadell methods respectively). The following roundability sequence is thus obtained: pyroxene > Fe-Ti-Cr oxides ≈ epidote ≥ amphibole > garnet ≥ zircon.

Shape Effects and Relative Rollability of Detrital Minerals

Beach placers are lag deposits formed when high-energy waves impact the shoreline, and coarser detrital minerals having smaller pivoting angles and projecting higher above the bed experience greater flow velocities and are thus selectively entrained offshore (Komar and Li 1988; Garzanti et al. 2009). Shape may also play a significant role (Winkelmolen 1982). However, there are contrasting views whether rounded "rollable" spheres are entrained more easily than angular ellipsoidal particles (Hattingh and Illenberger 1995; Komar and Li 1986), or smooth equant particles concentrate instead in placer lags because their low surface/weight ratio "*makes them profit less from the drag forces of the medium*" (Winkelmolen 1972, p. 184; Winkelmolen and Veenstra 1974), as observed in previous studies (MacCarthy 1933; Pettijohn and Lundahl 1943). Other studies denied selective transport by roundness and shape (McBride et al. 1996).

Our observations on Moçamedes Desert sands confirm the tendency of heavy-mineral-enriched lag deposits to be finer-grained than neutral sands of identical provenance, but failed to show a marked control by particle shape and "rollability" on the mineralogy of beach placers, an effect which may thus be considered as secondary—or neglected altogether—while modeling selective-entrainment processes.

Provenance Implications of Anomalous Size Relationships

Intrasample mineralogical variability (i.e., the difference in composition among the various size classes of a sediment sample) is controlled principally by settling equivalence (Rubey 1933). Ultradense minerals such as garnet, zircon, or Fe-Ti-Cr oxides are finer-grained and systematically enriched in finer classes, whereas less dense minerals

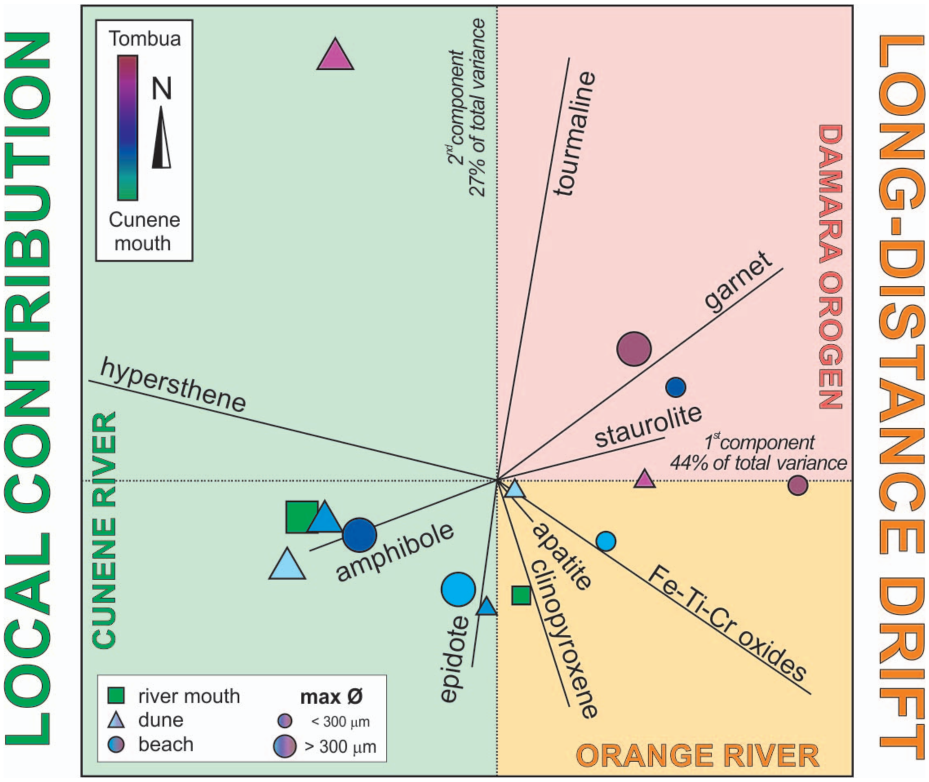

FIG. 9.—Intrasample mineralogical variability in Moçamedes Desert sand. In the compositional biplot (Gabriel 1971), all major heavy-mineral parameters are considered, and both multivariate observations (points) and variables (rays) are displayed. The length of each ray is proportional to the variability of the compositional parameter in the data set. If the angle between two rays is close to 0°, 90°, or 180°, then the corresponding parameters are directly correlated, uncorrelated, or inversely correlated, respectively. Commonly, rounded clinopyroxene and ultradense Fe-Ti-Cr oxide grains are concentrated in the finer mode (smaller symbols; Table A3), largely reflecting mechanical wear during long-distance multistep transport from the Orange mouth. Garnet, staurolite, and tourmaline tend to be coarser than expected because of both proximal supply from Damara basement rocks exposed in central and northern Namibia and greater toughness leading to more limited volume loss (Fig. 3A in Garzanti et al. 2015a). Angular amphibole and especially hypersthene supplied from the Cunene River are concentrated in the coarser mode (larger symbols) largely because of limited mechanical wear during short transport distances.

such as amphibole, quartz, and feldspars are concentrated in coarser classes (Garzanti et al. 2008). Exceptions to such physical rules may be caused by mixing of different grain populations with different provenance and grain size (e.g., Figs. 22 and 26 in Garzanti et al. 2015b). This is the case in the northern part of the Orange littoral cell, where garnet and staurolite grains—supplied largely from medium-grade metasedimentary rocks exposed in the Damara orogen of central Namibia—are coarser than less dense clinopyroxene because of both shorter transport and greater toughness leading to more limited loss and size reduction (Table 1; Fig. 3A in Garzanti et al. 2015a). This discrepancy is most evident in the Moçamedes Desert, where heavy-mineral data obtained by point-counting of the fine and coarse modes of the seven most markedly bimodal river, beach, and dune samples indicate a mixture of three mineralogically and texturally different grain populations (Fig. 9).

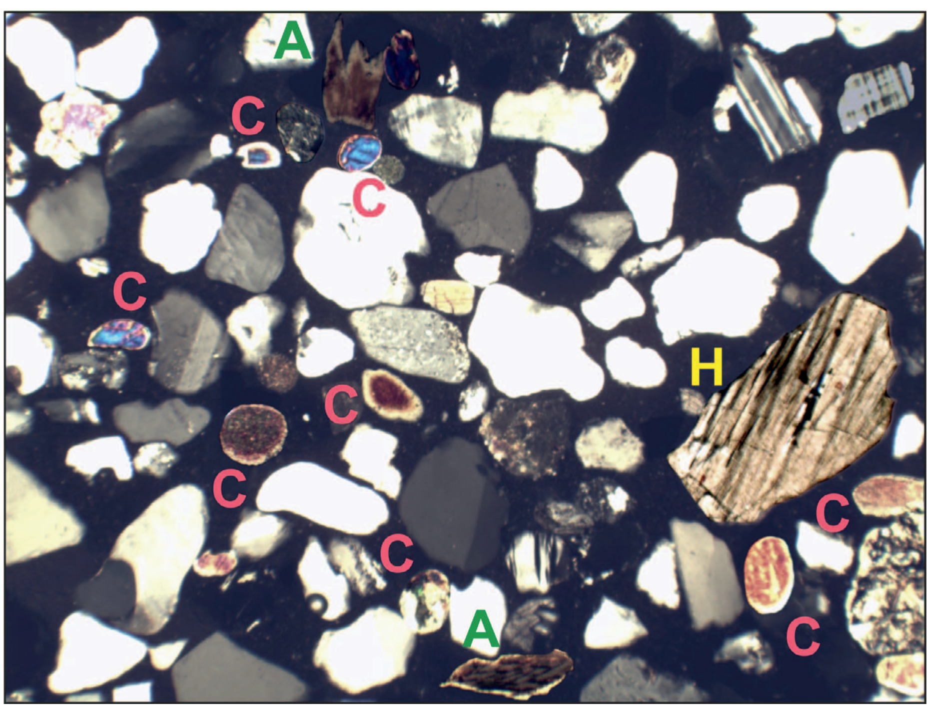

FIG. 10.—Mixed sediment provenance revealed by size and roundness anomalies. In beach sand at the Cunene River mouth, oversized subangular hypersthene (H) and angular corroded to skeletal amphibole (A) supplied locally by the Cunene River contrast with small subrounded to well rounded clinopyroxene (C) derived from the Orange river mouth after ultralong-distance northward transport through high-energy littoral and eolian environments.

Amphibole is coarser than expected in Moçamedes Desert sand, reflecting the local additional supply of coarser amphibole grains by the Cunene River. The Cunene River also supplies hypersthene, which in Moçamedes Desert sand samples is much coarser than clinopyroxene despite its slightly higher density (Fig. 9).

Provenance Implications of Anomalous Roundness Relationships

The most angular detrital minerals resulted to be garnet and staurolite, reflecting both their hardness and proximal provenance from the Damara orogen in central Namibia. The relatively high roundness of zircon already in the initial tract of the Orange littoral cell (Figs. 7, 8) suggests a largely recycled origin from Upper Carboniferous to Triassic sandstones of the Karoo Supergroup, extensively exposed in the Orange River catchment. Local provenance from the Cunene River is indicated by subangular hypersthene in dune and beach sands of the southern Moçamedes Desert, where amphibole is more angular than clinopyroxene (Fig. 10), reflecting supply in larger proportions from the Cunene and Swakop rivers as well as better cleavability.

CONCLUSIONS

In this article we have illustrated two methods to quantify grain roundness. To transfer faithfully into computer-based image analysis the original geometrical and graphical definitions used in sedimentology since Wadell (1932) and Krumbein (1941), we established a mathematical relationship between Fourier coefficients and Krumbein's visual scale and measured the difference between all corner-fitting circles and the maximum inscribed circle for all imaged grains. These two different approaches were applied to 22 selected samples of fluvial, eolian, and beach sands collected all along the longest cell of littoral transport documented on Earth, extending for 1800 km from the Orange mouth to southern Angola. This natural laboratory offers uniquely suitable conditions to investigate the effects of prolonged mechanical abrasion on textural parameters in different environments. Chiefly because of the difficulties involved not only in the objective definition and measurement of grain shape, but also in finding a suitable test case, this issue was scarcely explored by sedimentologists in the last decades, and has thus long remained controversial.

By monitoring mineralogical and textural trends throughout the Orange littoral cell we observed that the concentration, proportion, and size of heavy minerals do not change progressively with distance, although they do change markedly locally because of selective-entrainment effects or mixing with sediment supplied from subordinate river sources. This speaks against major effects of selective mechanical breakdown and also against systematic downdrift fining or downdrift sorting by density. The roundness of detrital minerals does not increase perceptibly during long-distance underwater transport, but does increase even within a short distance where grains pass from the marine to the eolian environment. This testifies to the much greater effectiveness of grain-to-grain impacts in air than in water. The obtained roundability sequence pyroxene $>$ Fe-Ti-Cr oxides $\approx$ epidote $\geq$ amphibole $>$ garnet $\geq$ zircon is broadly consistent with, and thus plausibly controlled by, increasing mineral hardness, confirming previous views. By comparing roundness of the same detrital mineral in placer, semi-placer, and anti-placer deposits, we also tested shape effects during selective entrainment, but we failed to find a significant correlation between rollability and roundness.

The critical evaluation of quantitative textural data provides fundamental complementary information to improve on our understanding of sediment-transport processes and sharpens the conceptual tools needed to detangle the multiple complexities found in source-to-sink studies.

SUPPLEMENTAL MATERIAL

Supplementary data associated with this article are available from JSR's Data Archive: http://sepm.org/pages.aspx?pageid=229, and includes full information on sampling sites (Table A1), data on textural properties (Table A2), and heavy-mineral assemblages (Table A3). Table captions and the flow chart describing the Wadell method are contained in Appendix A. The Google-Earth map of sampling sites *Roundness.kmz* is also provided. The Matlab™ script used to determine grain roundness is available at http://www.ighg.it/SedPetr/SEDPETR/software.html.

ACKNOWLEDGMENTS

Sampling in the field was carried out with Pieter Vermeesch, Pedro Dinis, João Huvi, Florian Kober, and Charlie Bristow, with fundamental logistic support from the University of Katyavala Bwila and Instituto Superior Politécnico da Tundavala. Additional samples were collected by Afonso Sampaio, Alcides Pereira, Fernand Vermeesch, and Dany Kerckhove. Danilo Controversio, Francesco Crotti, and Matteo Sala provided valuable help with image analysis. Careful constructive criticism by Reviewers Earle McBride and Mikael Attal, and advice by Editor Gary Hampson and Corresponding Editor John Southard are gratefully acknowledged.

REFERENCES

Attal, M., and Lavé, J., 2006, Changes of bedload characteristics along the Marsyandi River (central Nepal): implications for understanding hillslope sediment supply, sediment load evolution along fluvial networks, and denudation in active orogenic belts, *in* Willett, S.D., Hovius, N., Brandon, M.T., and Fisher, D., eds., Tectonics, Climate, and Landscape Evolution: Geological Society of America, Special Paper 398, p. 143–171.

Beddow, J.K., 1986, Size, shape, and texture analysis, *in* Ishizaka, S., ed., Science on Form: Proceedings of the First International Symposium for Science on Form, Tokyo, KTK Scientific Publishers, p. 201–218.

Beddow, J.K., Philip, G.C., Vetter, A.F., and Nasta, M.D., 1977, On relating some particle profile characteristics to the profile Fourier coefficients: Powder Technology, v. 18, p. 19–25.

Blatt, H., 1978, Sediment dispersal from Vogelsberg Basalt, Hessen, West Germany: Geologische Rundschau, v. 67, p. 1009–1015.

Bowman, E.T., Soga, K., and Drummond, T.W., 2000, Particle shape characterisation using Fourier analysis: University of Cambridge, Department of Engineering, CUED/D-Soils, TR315, p. 1–20.

Breyer, J.A., and Bart, H.A., 1978, The composition of fluvial sands in a temperate semiarid region: Journal of Sedimentary Petrology, v. 48, p. 1311–1320.

Cardinale, J., Paul, G., and Sbalzarini, I.F., 2012, Discrete region competition for unknown numbers of connected regions: Institute of Electrical and Electronics Engineers, Transactions on Image Processing, v. 21, p. 3531–3545.

Cascalho, J., and Fradique, C., 2007, The sources and hydraulic sorting of heavy minerals on the northern Portuguese continental margin, *in* Mange, M.A., and Wright, D.T., eds., Heavy Minerals in Use: Amsterdam, Elsevier, Developments in Sedimentology, v. 58, p. 75–110.

Cipriani, L.E., and Stone, G.W., 2001, Net longshore sediment transport and textural changes in beach sediments along the southwest Alabama and Mississippi barrier islands, USA: Journal of Coastal Research, v. 17, p. 443–458.

Clark, M.W., 1981, Quantitative shape analysis: a review: Mathematical Geology, v. 13, p. 303–320.

Cox, M.R., and Budhu, M., 2008, A practical approach to grain shape quantification: Engineering Geology, v. 96, p. 1–16.

Curray, J.R., and Griffiths, J.C., 1955, Sphericity and roundness of quartz grains in sediments: Geological Society of America, Bulletin, v. 66, p. 1075–1096.

Diepenbroek, M., Bartholomä, A., and Ibbeken, H., 1992, How round is round? A new approach to the topic "roundness" by Fourier grain shape analysis: Sedimentology, v. 39, p. 411–422.

Dietz, V., 1973, Experiments on the influence of transport on shape and roundness of heavy minerals, *in* Füchtbauer, H., Lisitzyn, A.P., Milliman, J.D., and Seibold, E., eds., Contributions to Sedimentology: Stuttgart, E. Schweizerbart, v. 1, p. 69–102.

Dill, H.G., 2007, Grain morphology of heavy minerals from marine and continental placer deposits, with special reference to Fe–Ti oxides: Sedimentary Geology, v. 198, p. 1–27.

Dobkins, J.E., and Folk, R.L., 1970, Shape development on Tahiti-nui: Journal of Sedimentary Petrology, v. 40, p. 1167–1203.

Domokos, G., Jerolmack, D.J., Sipos, A.Á., and Török, Á., 2014, How river rocks round: resolving the shape-size paradox: PLOS One, v. 9, e88657, doi:10.1371/journal.pone.0088657.

Dott, R.H., 2003, The importance of eolian abrasion in supermature quartz sandstones and the paradox of weathering on vegetation-free landscapes: The Journal of Geology, v. 111, p. 387–405.

Dutta, P.K., Zhou, Z., and dos Santos, P.R., 1993, A theoretical study of mineralogical maturation of eolian sand, *in* Johnsson, M.J., and Basu, A., eds., Processes Controlling the Composition of Clastic Sediments: Geological Society of America, Special Paper 284, p. 203–209.

Ehrlich, R., and Weinberg, B., 1970, An exact method for characterization of grain shape: Journal of Sedimentary Petrology, v. 40, p. 205–212.

Folk, R.L., 1951, A comparison chart for visual percentage estimation: Journal of Sedimentary Research, v. 21, p. 32–33.

Folk, R.L., 1955, Student operator error in determination of roundness, sphericity, and grain size: Journal of Sedimentary Petrology, v. 25, p. 297–301.

Folk, R.L., 1980, Petrology of Sedimentary Rocks: Austin, Texas, Hemphill Publishing, 182 p.

Frihy, O.E., and Komar, P.D., 1991, Patterns of beach-sand sorting and shoreline erosion on the Nile delta: Journal of Sedimentary Petrology, v. 61, p. 544–550.

Gabriel, K.R., 1971, The biplot graphic display of matrices with application to principal component analysis: Biometrika, v. 58, p. 453–467.

Garzanti E., 2017, The maturity myth in sedimentology and provenance analysis: Journal of Sedimentary Research, v. 87, p. 353–365.

Garzanti, E., Scutellà, M., and Vidimari, C., 1998, Provenance from ophiolites and oceanic allochthons: modern beach and river sands from Liguria and the Northern Apennines (Italy): Ofioliti, v. 23, p. 65–82.

Garzanti, E., Canclini, S., Moretti Foggia, F., and Petrella, N., 2002, Unraveling magmatic and orogenic provenances in modern sands: the back-arc side of the Apennine thrust-belt (Italy): Journal of Sedimentary Research, v. 72, p. 2–17.

Garzanti, E., Andò, S., and Vezzoli, G., 2008, Settling-equivalence of detrital minerals and grain-size dependence of sediment composition: Earth and Planetary Science Letters, v. 273, p. 138–151.

Garzanti, E., Andò, S., and Vezzoli, G., 2009, Grain-size dependence of sediment composition and environmental bias in provenance studies: Earth and Planetary Science Letters, v. 277, p. 422–432.

Garzanti, E., Andò, S., Vezzoli, G., Lustrino, M., Boni, M., and Vermeesch, P., 2012, Petrology of the Namib sand sea: long-distance transport and compositional variability in the wind-displaced Orange Delta: Earth-Science Reviews, v. 11, p. 173–189.

Garzanti, E., Limonta, M., Resentini, A., Bandopadhyay, P.C., Najman, Y., Andò, S., and Vezzoli, G., 2013, Sediment recycling at convergent plate margins (Indo-Burman Ranges and Andaman–Nicobar Ridge): Earth-Science Reviews, v. 123, p. 113–132.

Garzanti, E., Vermeesch, P., Andò, S., Lustrino, M., Padoan, M., and Vezzoli, G., 2014, Ultra-long distance littoral transport of Orange sand and provenance of the Skeleton Coast Erg (Namibia): Marine Geology, v. 357, p. 25–36.

Garzanti, E., Resentini, A., Andò, S., Vezzoli, G., and Vermeesch, P., 2015a, Physical controls on sand composition and relative durability of detrital minerals during long-distance littoral and eolian transport (coastal Namibia): Sedimentology, v. 62, p. 971–996.

Garzanti, E., Andò, S., Padoan, M., Vezzoli, G., and El Kammar, A., 2015b, The modern Nile sediment system: processes and products: Quaternary Science Reviews, v. 130, p. 9–56.

Garzanti, E., Dinis, P., Vermeesch, P., Andò, S., Hahn, A., Huvi, J., Limonta, M., Padoan, M., Resentini, A., Rittner, M., and Vezzoli, G., 2017a, Sedimentary processes controlling ultralong cells of littoral transport: placer formation and termination of the Orange sand highway in southern Angola: Sedimentology, doi: 10.1111/sed.12387.

Garzanti E., Vermeesch, P., Al-Ramadan, K.A., Andò, S., Limonta, M., Peters, G., Rittner, M., and Vezzoli, G., 2017b, Tracing transcontinental sand transport from the Anatolia–Zagros orogen to beyond the Gulf foreland-basin into the Rub' al Khali sand sea: Journal of Sedimentary Research, v. 87, p. 1196–1213.

Goudie, A.S., and Watson, A., 1981, The shape of desert sand dune grains: Journal of Arid Environments, v. 4, p. 185–190.

Harrell, J., 1984, A visual comparator for degree of sorting in thin and plane sections: Journal of Sedimentary Petrology, v. 54, p. 646–650.

Hattingh, J., and Illenberger, W.K., 1995, Shape sorting of flood-transported synthetic clasts in a gravel bed river: Sedimentary Geology, v. 96, p. 181–190.

Hryciw, R.D., Zheng, J., and Shetler, K., 2016, Particle roundness and sphericity from images of assemblies by chart estimates and computer methods: Journal of Geotechnical and Geoenvironmental Engineering, v. 142, doi:10.1061/(ASCE)GT.1943-5606.0001485.

Hyslip, J.P., and Vallejo, L.E., 1997, Fractal analysis of the roughness and size distribution of granular materials: Engineering Geology, v. 48, p. 231–244.

Ingersoll, R.V., Kretchmer, A.G., and Valles, P.K., 1993, The effect of sampling scale on actualistic sandstone petrofacies: Sedimentology, v. 40, p. 937–953.

Jacob, J., Ward, J.D., Bluck, B.J., Scholz, R.A., and Frimmel, H.E., 2006, Some observations on diamondiferous bedrock gully trapsites on Late Cainozoic, marine-cut platforms of the Sperrgebiet, Namibia: Ore Geology Reviews, v. 28, p. 493–506.

Jerram, D.A., 2001, Visual comparators for degree of grain-size sorting in two and three dimensions: Computers & Geosciences, v. 27, p. 485–492.

Kaye, B.H., 1978, Specification of the ruggedness and/or texture of a fine particle profile by its fractal dimension: Powder Technology, v. 21, p. 1–16.

Komar, P.D., and Li, Z., 1986, Pivoting analyses of the selective entrainment of sediments by shape and size with application to gravel threshold: Sedimentology, v. 33, p. 425–436.

Komar, P.D., and Li, Z., 1988, Application of grain-pivoting and sliding analyses to selective entrainment of gravel and to flow-competence evaluations: Sedimentology, v. 35, p. 681–695.

Krumbein, W.C., 1940, Flood gravel of San Gabriel Canyon, California: Geological Society of America, Bulletin, v. 51, p. 639–676.

Krumbein, W.C., 1941, Measurement and geological significance of shape and roundness of sedimentary particles: Journal of Sedimentary Petrology, v. 11, p. 64–72.

Krynine, P.D., 1956, Sphericity and roundness through the ages: Geological Society of America, Bulletin, v. 67, p. 1661.

Kuenen, P.H., 1959, Experimental abrasion: 3. Fluviatile action on sand: American Journal of Science, v. 257, p. 172–190.

Kuenen, P.H., 1960, Experimental abrasion: 4. Eolian action: The Journal of Geology, v. 68, p. 427–449.

Kuenen, P.H., 1964, Experimental abrasion: 6. Surf action: Sedimentology, v. 3, p. 29–43.

Leeder, M.R., 1982, Sedimentology, Process and Product: London, Allen & Unwin, 344 p.

Li, M.Z., and Komar, P.D., 1992, Longshore grain sorting and beach placer formation adjacent to the Columbia River: Journal of Sedimentary Petrology, v. 62, p. 429–441.

Luerkens, D.W., 1991, Theory and Application of Morphological Analysis: Fine Particles and Surfaces: Boca Raton, CRC Press, 304 p.

MacCarthy, G.R., 1933, The rounding of beach sands: American Journal of Science, v. 147, p. 205–224.

Mackie, W., 1897, On the laws that govern the rounding of particles of sand: Edinburgh Geological Society, Transactions, v. 7, p. 298–311.

Mandelbrot, B.B., 1977, Fractals: Form, Chance and Dimension: San Francisco, Freeman, 361 p.

Marsland, P.S., and Woodruff, J.G., 1937, A study of the effects of wind transportation on grains of several minerals: Journal of Sedimentary Petrology, v. 7, p. 18–30.

McBride, E.F., and Picard, D.M., 1987, Downstream changes in sand composition, roundness and gravel size in a short-headed, high-gradient stream, northwestern Italy: Journal of Sedimentary Petrology, v. 57, p. 1018–1026.

McBride, E.F., Abel-Wahab, A., and McGilvery, T.A., 1996, Loss of sand-size feldspar and rock fragments along the South Texas Barrier Island, US: Sedimentary Geology, v. 107, p. 37–44.

McCave, I.N., 1978, Grain-size trends and transport along beaches: example from eastern England: Marine Geology, v. 28, p. M43–M51.

Mehring, J.L., and McBride, E.F., 2007, Origin of modern quartzarenite beach sands in a temperate climate, Florida and Alabama, US: Sedimentary Geology, v. 201, p. 432–445.

Miller, K.L., Szabó, T., Jerolmack, D.J., and Domokos, G., 2014, Quantifying the significance of abrasion and selective transport for downstream fluvial grain size evolution: Journal of Geophysical Research, Earth Surface, v. 119, p. 2412–2429.

Muhs, D.R., 2004, Mineralogical maturity in dunefields of North America, Africa and Australia: Geomorphology, v. 59, p. 247–269.

Nesbitt, H.W., and Young, G.M., 1996, Petrogenesis of sediments in the absence of chemical weathering: effects of abrasion and sorting on bulk composition and mineralogy: Sedimentology, v. 43, p. 341–358.

Nixon, M.S., and Aguado, A.S., 2002, Feature Extraction and Image Processing for Computer Vision: Cambridge, Massachusetts, Academic Press, 360 p.

Orford, J.D., and Whalley, W.B., 1983, The use of the fractal dimension to quantify the morphology of irregular-shaped particles: Sedimentology, v. 30, p. 655–668.

Pettijohn, F.J., 1957, Sedimentary Rocks: New York, Harper and Brothers, 718 p.

Pettijohn, F.J., and Lundahl, A.C., 1943, Shape and roundness of Lake Erie beach sands: Journal of Sedimentary Petrology, v. 13, p. 69–78.

Pettijohn, F.J., and Ridge, J.D., 1932, A textural variation series of beach sands from Cedar Point, Ohio: Journal of Sedimentary Petrology, v. 2, p. 76–88.

Pettijohn, F.J., Potter, P.E., and Siever, R., 1973, Sand and Sandstone: New York, Springer, 618 p.

Picard, M.D., and McBride, E.F., 2007, Comparison of river and beach sand composition with source rocks, Dolomite Alps drainage basins, northeastern Italy, *in* Arribas, J., Johnsson, M.J., and Critelli, S., eds., Sedimentary Provenance and Petrogenesis: Perspectives from Petrography and Geochemistry: Geological Society of America, Special Paper 420, p. 1–12.

Popper, K., 1959, The Logic of Scientific Discovery: London, Hutchinson & Co, 480 p.

Powers, M.C., 1953, A new roundness scale for sedimentary particles: Journal of Sedimentary Petrology, v. 23, p. 117–119.

Raadnui, S., 2005, Wear particle analysis: utilization of quantitative computer image analysis: a review: Tribology International, v. 38, p. 871–878.

Rasband, W.S., 1997, ImageJ: Bethesda, Maryland, US National Institute of Health, https://imagej.nih.gov/ij/.

Rogers, J., 1977, Sedimentation on the continental margin off the Orange River and the Namib desert: Geology Survey/University of Cape Town, Marine Geosciences Group, Bulletin, v. 7, p. 1–162.

Rubey, W.W., 1933, The size-distribution of heavy minerals within a water-laid sandstone: Journal of Sedimentary Petrology, v. 3, p. 3–29.

Russell, R.D., 1937, Mineral composition of Mississippi River sands: Geological Society of America, Bulletin, v. 48, p. 1307–1348.

Russell, R.D., 1939, Effects of transportation on sedimentary particles: Part 1. Transportation, *in* Trask, P.D., ed., Recent Marine Sediments, a Symposium: Society of Economic Paleontologists and Mineralogists, Special Publication 4, p. 32–47.

Russell, R.D., and Taylor, R.E., 1937, Roundness and shape of Mississippi River sands: The Journal of Geology, v. 45, p. 225–267.

Savage, K.M., de Cesero, P., and Potter, P.E., 1988, Mineralogical maturity of modem sand along a high energy tropical coast: Baixada de Jacarepegua, Rio de Janeiro, Brazil: Journal of South American Earth Sciences, v. 1, p. 317–328.

Self, R.P., 1977, Longshore variation in beach sands Nautla area, Veracruz, Mexico: Journal of Sedimentary Petrology, v. 47, p. 1437–1443.

Shukri, N.M., 1950, The mineralogy of some Nile sediments: Geological Society of London, Quarterly Journal, v. 105, p. 511–534.

Sneed, E.D., and Folk, R.L., 1958, Pebbles in the lower Colorado River, Texas: a study in particle morphogenesis: The Journal of Geology, v. 66, p. 114–150.

Spaggiari, R.I., Bluck, B.J., and Ward, J.D., 2006, Characteristics of diamondiferous Plio-Pleistocene littoral deposits within the palaeo–Orange River mouth, Namibia: Ore Geology Reviews, v. 28, p. 475–492.

Sun, T.H., 2009, Applying particle swarm optimization algorithm: Expert Systems with Applications, v. 36, p. 3428–3438.

Tafesse, S., Fernlund, J.M.R., Sun, W., and Bergholm, F., 2013, Evaluation of image analysis methods used for quantification of particle angularity: Sedimentology, v. 60, p. 1100–1110.

Taubin, G., 1991, Estimation of planar curves, surfaces, and nonplanar space curves defined by implicit equations with applications to edge and range image segmentation: Institute of Electrical and Electronics Engineers, Transactions on Pattern Analysis and Machine Intelligence, v. 13, p. 1115–1138.

Terry, R.D., and Chilingar, G.V., 1955, Comparison charts for visual estimation of percentage composition: Journal of Sediment Petrology, v. 25, p. 229–234.

Thomas, M.C., Wiltshire, R.J., and Williams, A.T., 1995, The use of Fourier descriptors in the classification of particle shape: Sedimentology, v. 42, p. 635–645.

Twenhofel, W.H., 1945, The rounding of sand grains: Journal of Sedimentary Petrology, v. 15, p. 59–71.

Vallejo, L.E., and Zhou, Y., 1995, The relationship between the fractal dimension and Krumbein's roundness number: Soils and Foundations, v. 35, p. 163–167.

Vermeesch, P., Resentini, A., and Garzanti, E., 2016, An R package for statistical provenance analysis: Sedimentary Geology, v. 336, p. 14–25.

Wadell, H., 1932, Volume, shape, and roundness of rock particles: The Journal of Geology, v. 40, p. 443–451.

Wentworth, C.K., 1919, A Laboratory and field study of cobble abrasion: The Journal of Geology, v. 27, p. 507–521.

Whalley, W.B., and Orford, J.D., 1989, The use of fractals and pseudofractals in the analysis of two-dimensional outlines: review and further exploration: Computers & Geosciences, v. 15, p. 185–197.

Winkelmolen, A.M., 1972, Shape sorting in the lower Oligocene, northern Belgium: Sedimentary Geology, v. 7, p. 183–227.

Winkelmolen, A.M., 1982, Critical remarks on grain parameters, with special emphasis on shape: Sedimentology, v. 29, p. 255–265.

Winkelmolen, A.M., and Veenstra, H.J., 1974, Size and shape sorting in a Dutch tidal inlet: Sedimentology, v. 21, p. 107–126.

Xia, W., 2017, Role of particle shape in the floatability of mineral particles: an overview of recent advances: Powder Technology, v. 317, p. 104–116.

Zheng, J., and Hryciw, R.D., 2015, Traditional soil particle sphericity, roundness and surface roughness by computational geometry: Géotechnique, v. 65, p. 494–506.

Received 12 June 2017; accepted 27 November 2017.